Advances in Science and Technology Research Journal

Advances in Science and Technology Research Journal, 18(8), 319–332
https://doi.org/10.12913/22998624/194128
ISSN 2299-8624, License CC-BY 4.0

Received: 2024.09.03
Accepted: 2024.10.04
Published: 2024.11.01

Effect of Rockfos Material Granulation on Phosphorus Sorption Kinetics

Beata Zawadzka[1,2], Michał Marzec[1*], Tadeusz Siwiec[1], Krzysztof Jóźwiakowski[1]

[1] Department of Environmental Engineering, University of Life Sciences in Lublin, Leszczyńskiego 7, 20-069 Lublin, Poland

[2] Mirosław Zalewski MONT-SAN, Rogoźnica 75, 21-560 Międzyrzec Podlaski, Poland

* Corresponding author's e-mail: michal.marzec@up.lublin.pl

ABSTRACT

The objective of the study was to analyze the kinetics of phosphorus sorption on Rockfos® material in terms of its potential use in water and wastewater treatment. The objective of the study was to ascertain the sorption capacity of the material in relation to its granularity and the predominant sorption process during the removal of phosphorus on this material. The Rockfos® material is manufactured from opoka through a thermal treatment process at 900 °C. Tests were conducted on three granulations of the sorbent. The granulations were tested at sizes ranging from 1.0 to 1.6 mm, from 1.6 to 2.5 mm, and from 2.0 to 5.0 mm, using a synthetic solution with a phosphorus content of 1.0 mg/L. The kinetics of phosphorus sorption were analyzed using a variety of kinetic models, including the pseudo-first-order (PFO), pseudo-second-order (PSO), Webber-Morris (W-M), and Elovich (E) models. The degree of fit between the various models and the results of the measurements was evaluated based on an error analysis. The results demonstrated that the pseudo-second-order kinetic model provided the most accurate description of the sorption process on Rockfos® material. This finding suggests that phosphorus sorption is primarily governed by the chemisorption process. The sorption rate constant exhibited the highest value for granulations of 1.6–2.5 mm and the lowest for granulations of 2.0–5.0 mm. The sorption capacity did not exceed 0.05 mg/g in any case, with the highest value observed for material granulations of 2.0–5.0 mm and the lowest observed for grains of 1.0–1.6 mm. The phosphorus removal effects from solution for granulations of 1.0–1.6 mm, 1.6–2.5 mm, and 2.0–5.0 mm were 74.3%, 92.4%, and 97.1%, respectively. These values were positively correlated with pH value.

Keywords: wastewater treatment; phosphorus removal; Rockfos material®, sorption kinetics.

INTRODUCTION

Modern technologies for phosphorus removal from wastewater and water are based on adsorption and precipitation processes [1, 2]. Adsorption technology is economical, simple and highly effective in removing phosphate from wastewater even at low concentrations [3-6] It involves the binding of molecules, atoms or ions on a surface or physical phase boundary. The center of the adsorption process as a surface phenomenon is usually a porous solid medium in which a multicomponent liquid (liquid or gas) mixture is attracted to the solid surface by chemical or physical bonds [7]. Adsorption is a complex process and largely dependent on the type of adsorbent used, and in particular the functional groups present on its surface [1, 7]. A decisive feature of the adsorbent's suitability is the large number of micropores and their well-developed network, allowing adsorbate molecules to enter the adsorbent [8, 9]. A potential material for phosphorus removal from wastewater or water should contain compounds capable of binding phosphorus, such as Ca, Mg, Fe and Al [1, 10]. In line with the concepts of green chemistry and

sustainable development (ecogreen), low-cost and environmentally friendly materials are being sought as adsorbents for phosphorus [11, 12]. Currently, natural or waste materials modified to produce a product with high phosphorus removal efficiency are widely used, including Leca®, Polonite®, Pollytag®, Filtralite® and Filtra P [1]. An important group in this regard is made up of materials produced on the basis of opoka, including Rockfos®. Its potential for phosphorus removal is related to the original characteristics of the opoka rock, namely its high content of aluminum, iron, magnesium and mainly calcium [13–17]. It is formed by decarbonation (high-temperature firing) of the opoka, which breaks down calcium carbonate to calcium oxide and carbon dioxide, making the material much more reactive toward phosphorus than opoka in its natural state [1, 18–20]. Preliminary results of laboratory tests [15, 17, 20–22], as well as field [23, 24] have shown that it is a very promising material for the removal and recovery of phosphorus from wastewater. In laboratory tests, more than 90% phosphorus reduction from wastewater was achieved with sufficiently long contact time [20]. In contrast, preliminary experiments conducted on a full technical scale have shown phosphorus removal efficiencies of about 40% [23, 24]. The efficiency of phosphorus sorption depends on the operating conditions, the nature of the flow and the contact time of the wastewater with the sorption material, which can be shaped taking into account the current economic and technical possibilities, however, a very important factor is the sorption capacity of the adsorbent. Previous studies of the sorption kinetics of Rockfos® material have yielded very divergent results. The sorption capacity of the fine fraction (0–2 mm) determined in tests with real wastewater and at low phosphate concentration was 0.9 mg/g [17]. Using synthetic wastewater with higher phosphate concentrations, the sorption capacity was determined to be 9.6 mg/g and 45.6 mg/g, while the theoretical maximum sorption capacity from the Langmuir model could reach 256 mg/g [22]. For material granulation of 2–8 mm, the sorption capacity was 0.36 mg/g [21]. Under the assumption of constancy in the chemical composition of the adsorbent, such a large variation in results could have been influenced by factors related to the organization of the experimental work, the chemical composition of the wastewater and solutions, or the adopted granulation of the adsorbent and the specific surface area of phosphate binding [17, 22].

Accordingly, kinetics studies of phosphorus sorption on Rockfos® material were carried out to determine the speed of the process and the sorption capacity of the material depending on its granularity under established conditions. Kinetics studies make it possible to determine the speed of the process, the maximum adsorbent absorption capacity and, on this basis, to assess the possibility of determining the type of adsorption dominant during phosphorus removal on Rockfos® material. Experimental kinetic data of total phosphorus adsorption on Rockfos® material were fitted to pseudo first-order (PFO), pseudo second-order (PSO) and Webber-Morris (W-M) and Elovich (E) kinetic models. Error analysis was used to assess the degree of fit of the various models to the measurement results. Determining the relationship between the pH value and the rate of phosphorus reduction was also an important part of the research conducted. The results of the study, including kinetic models of adsorption, can provide important information on the performance of adsorbents under specific conditions and be used in the planning and design of full-scale technical adsorption processes.

MATERIALS AND METHODS

Adsorbent

The Rockfos® material is produced on the basis of the opoka rock, which is mined near Piaski, in the Lublin Province. The material is created by heat treatment of the rock at 900°C. Rockfos® material has a porosity of 54%. It is characterized by a high content of CaO at 43.336% by weight and SiO_2 - 36.047%. The chemical composition of the material is described in detail in [18, 23, 24]. The reaction of the material is alkaline, and its pH is 11–12.

Phosphorus sorption kinetic models were determined for three sorbent granulations: 1.0–1.6 mm, 1.6–2.5 mm and 2.0–5.0 mm. Rockfos® material was sieved through sieves of the appropriate granulation and washed several times with water to remove particles adhering to the surface, then dried in a laboratory dryer at 100 °C for 8 hours.

Aqueous solution of phosphate

A stock solution of synthetic phosphate was prepared at a concentration of 50.00 mg/L by dissolving 0.220 g of analytical grade anhydrous potassium dihydrogen phosphate (KH_2PO_4) in distilled water in a 1,000-mL volumetric flask. Subsequently,

the stock solution was diluted with distilled water to achieve the requisite concentration of the experimental working solution (i.e., 1.00 mg/L).

Analytical methods

The sorption kinetics studies were carried out in a set of Erlenmayer flasks (200 ml) in which a fixed mass of sorbent was weighed, viz: 2,000 g with granulations: 1.0–1.6, 1.6–2.5, 2.0–5.0 mm. To each series of flasks, 100 ml of solution with phosphorus concentration of 1.00 mg/L was added. The samples were shaken in a laboratory shaker for 1 min to 48 h, at 20 °C. After the specified contact time (i.e. 1, 2, 5, 10, 15, 30, 60, 120, 180, 240, 360, 420, 720, 1440, 2160, 2880 min), the solutions were filtered on a paper filter. Aqueous samples were taken from the filtrate and their total phosphorus content was determined. Each series of tests was conducted in triplicate, and the arithmetic mean of the results was used for calculations. Total phosphorus was determined by spectrophotometric method with oxidation of the test sample in a thermoreactor at 120 °C for a period of 30 minutes, based on the international standard PN-EN ISO 6878: 2006 para. 8 Ap1:2010+Ap2:2010 [25]. Total phosphorus concentrations were measured using a NANOCOLOR® UV-VIS spectrophotometer (Macherey-Nagel, Düren, Germany). The pH value was also measured in each sample using an ORION Star A329 multi-parameter meter (Thermo Scientific, Waltham, USA). The pH values were measured in accordance with the international standard PN-EN ISO 10523: 2012 [26].

The amount of adsorbed PO_4^{3-} w after time t was calculated using the formula Eq. 1 [27–31]:

$$q_e = \frac{(C_0 - C_t)}{m} \cdot V \quad (1)$$

where: q_e - sorption capacity [mg/g]; C_0 and C_t - concentrations of PO_4^{3-} in the liquid phase before sorption and after time t [mg/L], respectively; V - volume of solution [L]; m - mass of dry adsorbent [g].

Kinetic models

Phosphorus sorption kinetics was analyzed based on four kinetic models: pseudo-first-order (PFO) and pseudo-second-order (PSO), Webber-Morris (W-M) and Elovich (E). Lagergren's PFO kinetic model describes the adsorption process at the solid-liquid interface. It is expressed by two equations: General form Eq. 2 and in linear form Eq. 3:

$$q = q_e(1 - e^{-k_1 t}) \quad (2)$$

$$ln\frac{(q_e - q)}{q_e} = -k_1 t \quad (3)$$

where: t - time [min]; q - the amount of adsorbate bound by the adsorbent at time t [mg/g]; q_e - the amount of adsorbate bound by the adsorbent at equilibrium [mg/g]; k_1 - process rate constant in the pseudo-first-order model [1/min].

Based on the graph and the equation of linear form of the PFO model, the constant parameters of the model were determined, such as the reaction rate constant (k_1), the sorption capacity (q_e), the coefficient of determination (R^2) and Pearson's correlation coefficient (r) Eq. 4.

$$r = \frac{\sum(x - \bar{x})(y - \bar{y})}{\sqrt{\sum(x - \bar{x})^2 \sum(y - \bar{y})^2}} \quad (4)$$

where: x - variable x; $\bar{x}$ - arithmetic mean of the x variable; y - y variable; $\bar{y}$ - arithmetic mean of the y variable.

The kinetic model (PSO) describes the rate of the adsorption process with respect to the difference between the equilibrium and current amount of adsorbate adsorbed. The PSO kinetic model is also represented by two equations: general form Eq. 5 and linear form Eq. 6 [22].

$$q = \frac{q_e^2 \cdot k_2 \cdot t}{1 + q_e \cdot k_2 t} \quad (5)$$

$$\frac{t}{q} = \frac{t}{k_2 \cdot q_e^2} + \frac{1}{q_e} \cdot t \quad (6)$$

where: t - time [min]; q - the amount of adsorbate bound by the adsorbent at time t [mg/g]; q_e - the amount of adsorbate bound by the adsorbent at equilibrium [mg/g]; k_2 - process rate constant in the pseudo-second-order model [g/mg·min].

Based on the graph and the equation of linear form of the PSO model, the constant parameters of the model were determined, such as the reaction rate constant (k_2), the sorption capacity (q), the coefficient of determination (R^2) and the correlation coefficient (r) Eq. 4.

The W-M model can indicate the presence of an intramolecular diffusion mechanism and was described by Eq. 7 [32]:

$$q_t = K_t \cdot t^{\frac{1}{2}} + C \quad (7)$$

where: K_t is the velocity constant of the intraparticle diffusion. The value of C indicates the boundary layer thickness. It corresponds to the intercept value.

In this model, if the curve q_t as a function of $t^{1/2}$ represents a straight line passing through the origin of the coordinate system, the speed of the adsorption phenomenon is considered to be limited by the intraparticle diffusion process [33]. As noted by Tsibranska and Hristova [34] the existence of different mass transfer mechanisms is manifested by different slopes in the linear plot of q_t against $t^{1/2}$, obtained by the method of sectional linear regression. They correspond to different, successive stages of mass transport with decreasing speed overcoming the different stages of the external part, followed by transfer and intraparticle diffusion in the macro-, meso- and microporous structure of the adsorbent. Hence, in the W-M model, the linear relationship is often divided into 2–3 separate sections with different slopes describing different diffusion rates [35].

The E model assumes that real surfaces of solids are energetically inhomogeneous and that neither desorption nor interactions between adsorbed substances can significantly affect adsorption kinetics at low surface coverage [36] and that the surface of the solid is energetically heterogeneous [36]. This model is described by Eq. 8 [37, 38].

$$q_t = \frac{1}{\beta} \cdot \ln(\alpha \cdot \beta) + \frac{1}{\beta} lnt \tag{8}$$

where: α is the initial sorption rate (mg/g·min), and the parameter β is related to the extent of surface coverage and activation energy for chemisorption (g/mg) [39].

Unfortunately, in the literature it is not given in a consistent form, you can find this model in other versions, for example, instead of the multiplier $1/\beta$, you can find the multiplier β [36], and in double logarithmic form [40].

Assessing the degree of fit of models

The analysis of the fit of measurement points and individual models was performed using the coefficient of determination R^2, the sum of squares of errors ERRSQ (the sum square of errors), the composite fractional error function HYBRD (hybrid fractional error function), the average relative error ARE (average relative error), the Fisher F test and the test χ^2 [41]. The relevant formulas are shown below.

$$ERRSQ = \sum_{i=1}^{k} \left(q_{exp} - q_{calc}\right)^2 \tag{9}$$

$$HYBRD = \frac{100}{k-p} \sum_{i=1}^{k} \left(\frac{\left(q_{exp} - q_{calc}\right)^2}{q_{exp}} \right) \tag{10}$$

$$ARE = \frac{100}{k} \sum_{i=1}^{k} \left| \frac{q_{exp} - q_{calc}}{q_{exp}} \right| \tag{11}$$

$$F = \frac{(k-p) \cdot \sum_{i=1}^{k} \left(q_{exp} - \frac{1}{k} \cdot \sum_{i=1}^{k} q_{exp} \right)^2}{(k-1) \cdot \sum_{i=1}^{k} \left(q_{exp} - q_{calc}\right)^2} \tag{12}$$

$$\chi^2 = \sum_{i=1}^{k} \left(\frac{\left(q_{exp} - q_{calc}\right)^2}{q_{calc}} \right) \tag{13}$$

where: q_{exp} - sorption obtained from measurements, q_{calc} - sorption obtained from calculations using the model in general form, k - number of measurement points, p - number of model parameters

RESULTS AND DISCUSSION

Phosphorus removal efficiency

During the study, a significant effect of Rockfos® material granulation on the degree of phosphorus reduction was observed. As shown in Figure 1, the highest degree of reduction was obtained for granulations of 2.0–5.0 mm and amounted to 97.1%. For the other granulations, i.e. 1.0–1.6 mm and 1.6–2.5 mm, the value was 74.3 % and 92.4 %, respectively. At the initial stage of the adsorption process, there was a rapid increase in the number of adsorbed particles, especially for the 1.0-1.6 mm and 1.6–2.5 mm fractions. After 10 minutes, the phosphorus removal rate was 16.5% and 23.0%, respectively. For the 2.0–5.0 mm granulation, after 10 minutes the degree of P reduction is only 7.8%. Increasing the contact time resulted in a regular increase in the phosphorus reduction rate After 240 minutes of contact, the reduction rate for individual fractions starting with the finest was already about 44.5%, 64% and 49.0% (Figure 1). For the 1.0–1.6 mm and 1.6-2.5 mm granulations, as the contact time increased, the adsorption rate decreased until the system reached dynamic equilibrium. On the other hand, for the 2.0–5.0 mm fraction, there was a further increase in the reduction rate, and after 720 minutes it was 87.9%. Equilibrium phosphorus removal for all three granulations was observed after 1440 minutes. The longer contact time between adsorbent and adsorbate did not affect the significant increase in phosphorus reduction. The

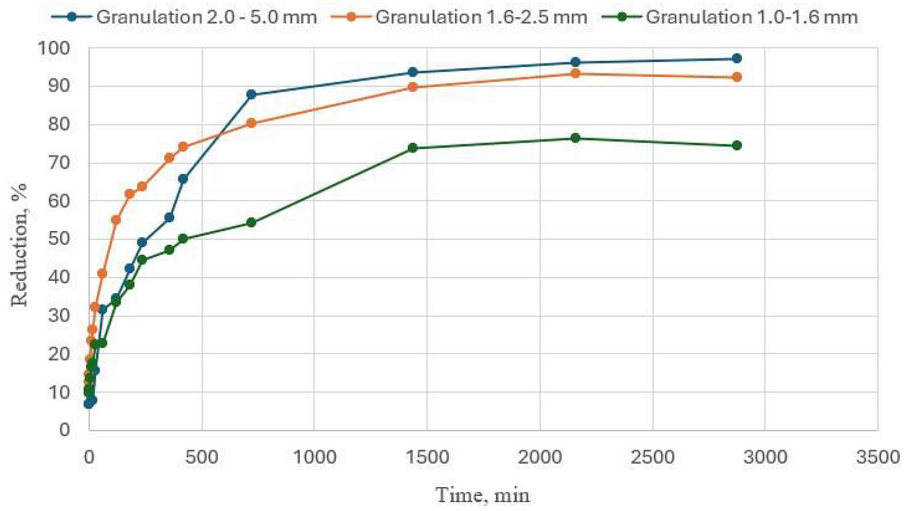

Figure 1. Reduction of total phosphorus over time for different Rockfos® granulations

rapid course of the adsorption process in the first stage is related to the large number of available active sites on the adsorbent surface capable of adsorbing phosphorus. On the other hand, in the next stage, the slowing down of adsorption may be due to saturation of active sites and due to repulsive forces between adsorbate particles adsorbed on the surface of the adsorbent and particles present in solution.

Kasprzyk et al. [21], analyzing two fractions of Rockfos® material using synthetic solutions found a slightly different trend. Phosphorus removal efficiencies for the 2.0–8.0 mm granulation ranged from 2.9 to 6.0 percent for phosphorus concentrations in solution in the range of 5–100 mg/L. At the same concentrations of phosphorus in solution, the phosphorus removal effects in material with a granulation of 0.0–2.0 mm oscillated between 94.7–97.8%. It is worth mentioning that these measurements, however, were performed under slightly different conditions, i.e. after 5 minutes of mixing the adsorbent sample with the solution and 1 hour of sedimentation [21].

Kinetics of sorption

Experimental kinetic data of adsorption of total phosphorus on Rockfos® material were fitted to kinetic models. Figure 2 shows the results to the PFO and PSO model and Figure 3 to the W-M and E model for this material with granulations of 1.0–1.6 mm, 1.6–2.5 mm and 2.0–5.0 mm.

Table 1 shows the determined, for all three granulations, kinetic parameters of the PFO model and PSO model in Table 2 for the W-M model, and in Table 3 for the E model.

The PFO kinetic model fits relatively well only for the finest fraction of 1.0–1.6 mm, as evidenced by the high R^2, above 0.9. The Pearson correlation coefficient for each granulation of Rockfos® material indicates a strongly negative correlation between sorption time and $\ln(q\text{-}q_{et})$. The highest equilibrium adsorption capacity was obtained from the PSO model for granulations 2.0–5.0 mm and was 0.0368 mg/g.

Accurate determination of q_e especially in the case of PFO is not easy, as in many cases the influence of physical adsorption and chemisorption causes further adsorbate binding to be very slow after an initially fast reaction, that it is difficult to determine whether equilibrium has been reached or not [36]. For many adsorption processes, the pseudo-first-order Lagergren model proves to be suitable only for the initial 20–30 minutes of interaction and is not suitable for the entire range of contact times [42].

The PSO kinetic model shows good agreement with the obtained results for each granulation of Rockfos® material. The linear determination coefficients R^2 reach high values above 0.99, which indicates a very good fit of the obtained experimental values to the pseudo-second-order model (Table 1). This is consistent with the theses of Ho and McKay [43], who analyzed kinetic data of sorption in the solid-liquid system and showed that in most cases the rate of the sorption process is well described by the pseudo-second-order equation. Kasprzyk et al. [22] using Rockfos® material with a granulation of 0.0–2.0 mm also

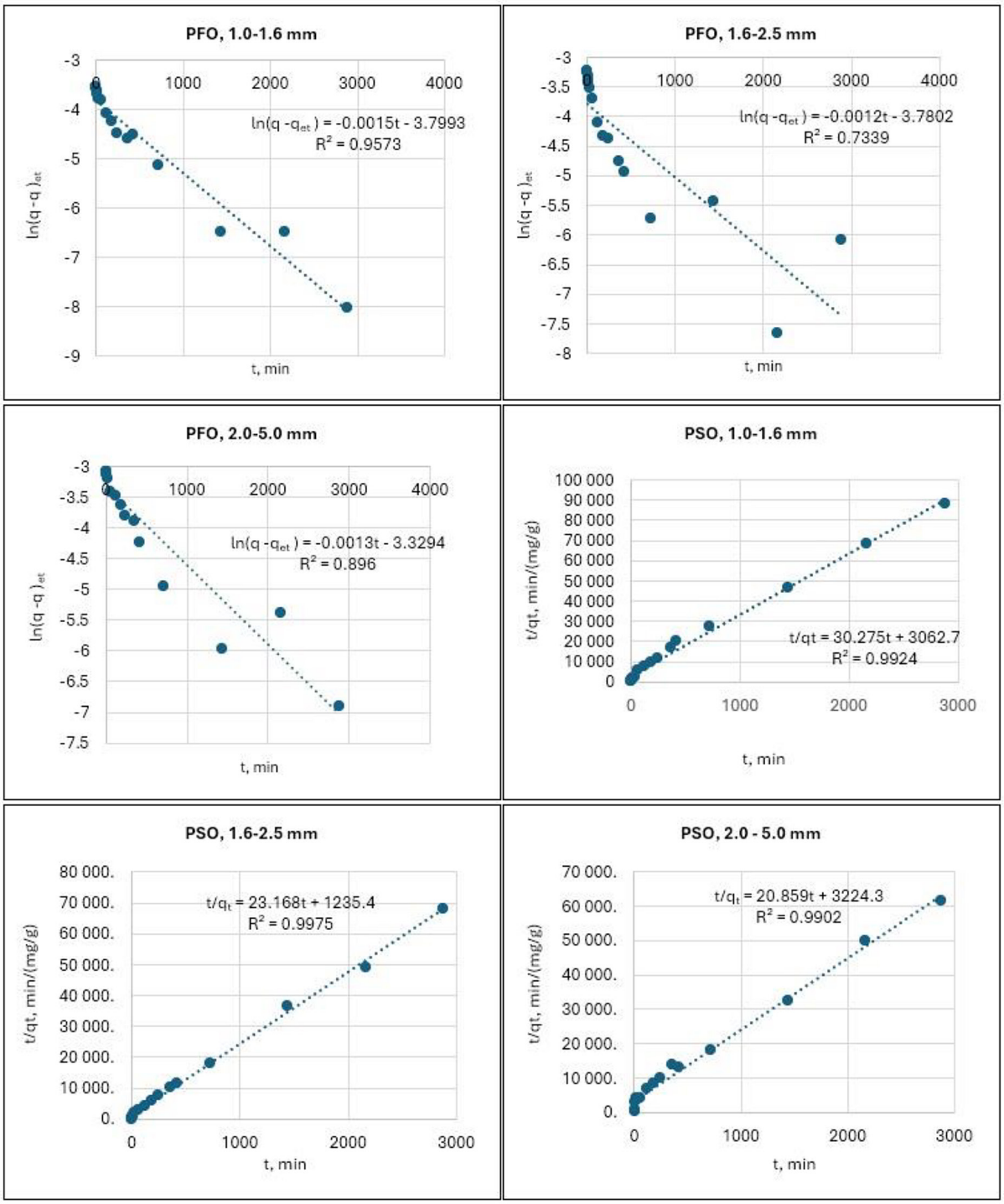

Figure 2. Adsorption kinetics for pseudo-first and pseudo-second order model of PO_4^{3-} on Rockfos® with a granulation of 1.0–1.6 mm, 1.6–2.5 mm and 2.0–5.0 mm

showed that the PSO model best describes the kinetics of phosphorus sorption. A similar pattern of phosphorus sorption kinetics was observed for the Polonite® material, which is produced on the basis of opoka [44] or other natural adsorbents such as sawdust, soil, rice husks, marble dust or palm fibers [45–48]. The high values of correlation coefficients obtained in the study by Jucherski et al. [20] also confirm the fit to a pseudo-second-order kinetic model.

Fitting the experimental results to a pseudo-second-order kinetics model suggests that phosphorus sorption on Rockfos® scales is based on a chemisorption process [43, 49]. During it, ionic or covalent chemical bonding occurs between adsorbate molecules and specific functional groups

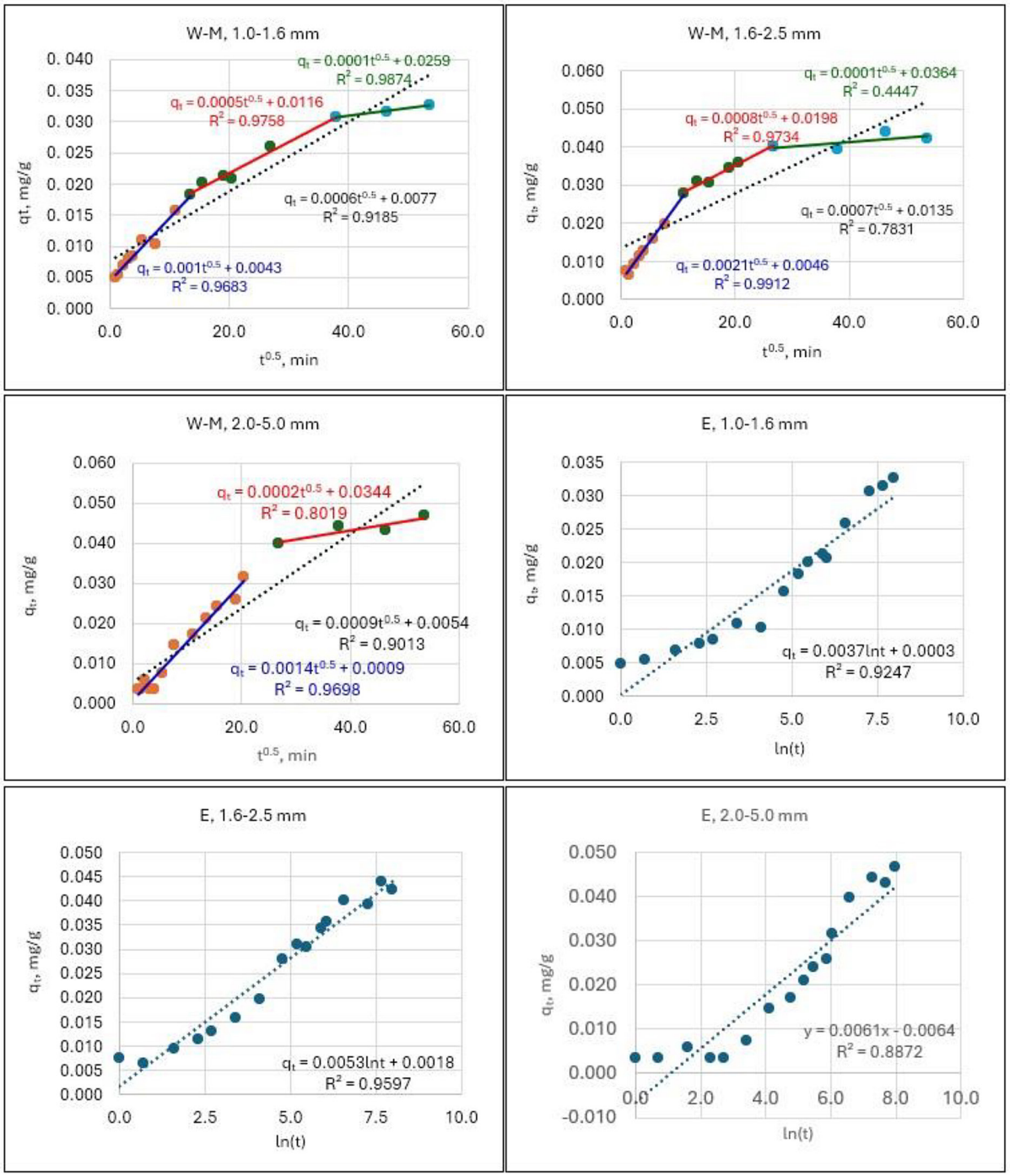

Figure 3. Adsorption kinetics for Webber-Morris and Elovich model of PO_4^{3-} on Rockfos® with a granulation of 1.0-1.6 mm, 1.6-2.5 mm and 2.0-5.0 mm

located on the surface of the adsorbent, resulting in a change in the electron configuration of both the adsorbate and the adsorbent [50, 51]. These bonds are strong and highly specific, and the main feature of chemisorption is its irreversible and selective nature. [52].

The equilibrium adsorption capacity obtained from the PSO model was highest for granulations of 2.0–5.0 mm (0.0479 mg/g), a slightly lower value was obtained for granulations of 1.6–2.5 mm (0.0432 mg/g). To date, many studies have been carried out on phosphorus sorption on natural and modified opoka, which are the starting material for Rockfos® [1, 13, 53–57]. Using synthetic solutions containing phosphorus, it was confirmed that thermal treatment significantly increased the sorption capacity due to the presence of calcium carbonate decomposition

Table 1. Kinetic parameters for pseudo-first and pseudo-second order model for the phosphates adsorption

Granulation, mm	Pseudo-first order model				Pseudo-second order model			
	q_e, mg/g	k_1, 1/min]	R^2	r	q_e, mg/g	k_2, g/mg·min	R^2	r
1.0-1.6	0.0229	0.00101	0.947	-0.973	0.0330	0.2993	0.992	0.996
1.6-2.5	0.0247	0.00094	0.764	-0.874	0.0432	0.4345	0.997	0.999
2.0-5.0	0.0368	0.00102	0.901	-0.949	0.0479	0.1349	0.990	0.995

Table 2. Kinetic parameters for Webber-Morris model for the phosphates adsorption

Parts of models	Parameters	Granulation, mm		
		1.0–1.6	1.6–2.5	2.0–5.0
Entire	K_{WM}, mg/g·min$^{1/2}$	0.0006	0.0007	0.0009
	C, mg/g	0.0077	0.0135	0.0054
	R^2, –	0.919	0.783	0.901
Phase I	K_{WM}, mg/g×min$^{1/2}$	0.001	0.0021	0.0014
	C, mg/g	0.0043	0.0046	0.0009
	R^2, –	0.968	0.991	0.970
Phase II	K_{WM}, mg/g·min$^{1/2}$	0.0005	0.0008	0.0002
	C, mg/g	0.0116	0.0198	0.0344
	R^2, –	0.919	0.973	0.802
Phase III	K_{WM}, mg/g·min$^{1/2}$	0.0001	0.0001	–
	C, mg/g	0.0259	0.0364	–
	R^2, –	0.987	0.445	–

Table 3. Kinetic parameters for Elovich model for the phosphates adsorption

Granulation, mm	α g/mg	β mg/g·min	R^2 –
1.0-1.6	0.0229	0.00101	0.947
1.6-2.5	0.0247	0.00094	0.764
2.0-5.0	0.0368	0.00102	0.901

products such as calcium oxide and carbon dioxide. Brogowski and Renman [53], showed that the heating process of the opoka increased the sorption capacity of PO_4 -P up to 119.6 mg/g for a heating temperature of 1000 °C. An even higher sorption capacity of opoka roasted at 900 °C was found by Cucarella et al. [54], 181.81 mg/g. For natural, non-calcined opoka, the sorption capacities were noticeably lower, from as low as 0.1 mg/g [58] to 19.6 mg/g [53].

Rockfos® material has been subjected to few tests for its sorption capacity. Kasprzyk et al. [22] determined the equilibrium adsorption capacity of phosphorus on Rockfos® material with a granulation of 0.0–2.0 mm to be 4.5 mg/g. An earlier study by Kasprzyk et al. [21], showed that the sorption capacity of this material varies quite a bit, and reaches levels ranging from 0.03 to 9.6 mg/g, depending on the granulation of the material and the properties of the solution.

The results presented in this paper show a significantly lower sorption capacity of Rockfos® material compared to literature data. The reason may be the initial concentration of phosphorus in solution, taken at a very low level of 1 mg/L. Meanwhile, according to the results of Kasprzyk et al. [21] there may be a positive correlation between the sorption capacity of the material and the concentration of phosphorus in solution.

According to the results presented in the literature, the higher phosphorus adsorption capacity of the Rockfos® material may be related to the very fine granulation (powder fraction), which gives a large specific surface area for phosphate binding [21, 53, 54]. In the present study, this thesis was not confirmed, and the granulation of 1.0–1.6

mmm had the lowest sorption capacity in both the pseudo-first-order and second-order kinetic models (Table 1). Literature data also indicate a positive correlation between the sorption capacity of Rockfos® material and the initial concentration of total phosphorus in solution [17, 22].

The granulation size of the Rockfos® material shows an effect on the speed of the sorption process. The pseudo-second-order rate constant k_2 reached the highest value for Rockfos® material with a granulation of 1.6-2.5 mm. However, the lowest value of k_2 was obtained for granulations of 2.0-5.0 mm. These values are significantly related to the mechanism of phosphorus sorption, with a smaller granulation of the material, more active sites are available, thus increasing the reaction rate.

The course of individual sorption steps in the W-M model does not give a clear answer regarding the size of sorbent grains. According to this model [32], when the graph of q_t as a function of $t^{1/2}$ results in a straight line passing through the origin of the coordinate system, the rate of the sorption process can be considered to be limited by the intraparticle diffusion process. Since this is not the case here, three-line diagrams for granulations of 1.0–1.6 mm and 1.6–2.5 mm and a two-line diagram for granulations of 2.0–5.0 mm were produced. In this case, it should be assumed that the adsorption process is not controlled solely by the intraparticle diffusion stage, but occurs in more stages. The initial stage (red markings) represents the influence of the boundary layer with external mass transfer. After about 180 minutes, adsorption (1.0–1.6 mm) and 120 minutes (1.6–2.5 mm) decreased, resulting in a second phase that lasted until, respectively, 1440 minutes and 720 minutes. This is probably diffusion to the inner parts of the adsorbent. Equilibrium was reached in the third phase, which led to a decrease in intramolecular diffusion, due to less availability of adsorption sites. Comparing the three diffusion constants of the Weber-Morris model, it can be concluded that $K_{W\text{-}M}$ is decreasing in successive phases, i.e. the diffusion of molecules inside the adsorbent is the decisive step in the adsorption process, as confirmed by the smallest value in the third phase.

The linear Elovich model (Fig. 3) did not correlate very well with the test results. The kinetic constants and coefficient of determination are shown in Table 3. Despite the high values of R^2, the arrangement of test points is clearly linear at first, and curvilinear in the later part. The analysis of a number of studies has observed that with a long testing time there is an unphysical behavior of the model equation *E*, which is due to the neglect of the rate of simultaneous desorption. Thus, in practice, the applicability of the Elovich equation is limited to the initial part of the adsorbate-adsorbent interaction process, when the system is relatively far from equilibrium state [36]. The Elovich equation is satisfied in chemical adsorption processes and is suitable for systems with heterogeneous adsorption surfaces [59]. An important part of the model is the proper determination of the time constant t_0 measurements and so if it is too small the curve is convex if too large it is concave [60].

In order to ascertain the precise fit of individual functions to the measurement results, error functions were established as optimization criteria. The characteristic quantities were determined using the formulas presented in Eq. (4, 9-13) and are presented in Table 4. The values presented in Table 4 were derived using the general formula as a foundation, free from the inherent inaccuracies associated with linearization and approximation.

Table 4 illustrates that the individual fit scores are not equally sensitive. The determination coefficients R^2 and Pearson's correlation coefficient *r*, as well as the results of Fisher's test, indicate that the larger their value, the better the fit they show. The remaining variables, namely *ESRQ, HYBRD, ARE*, and c^2 in such a case, the values should be as small as possible. The evaluation of the optimal kinetic fit model, which is based solely on the linear regression coefficient, may be susceptible to inaccuracy. Consequently, the necessity for supplementary statistical measures arises. It is observed that the greater the agreement between the adsorbed experimental phosphorus mass, designated as "q," and the calculated value, the closer the resulting statistical tool values are to the expected values, and thus the better the model. The model can be ordered in descending order of the cases with the highest values of the measures. The order of preference is as follows: PSO > W-M > E > PFO.

As can be seen, the R^2 values for PSO range from 0.99 to unity, demonstrating the best fit by PSO, suggesting a mechanism of chemisorption [61]. The use of disparate models and their evaluation is justified by the rarity of homogeneous sorbent surfaces and the frequent inseparability of the effects of transport phenomena and chemical reactions in experimental settings.

Table 4. Evaluation of the fit of kinetic models to experimental data

Granulation, mm	Model	R^2	*R (Pearson)*	*ESRQ*	*HYBRD*	*ARE*	*Fisher*	c^2
1.0-1.6	PFO	0.957	-0.973	2.11×10^{-3}	0.850	25.9	0.706	2.15
	PSO	0.992	0.996	2.19×10^{-4}	0.169	80.8	5.89	0.140
	W - M	0.919	0.958	1.31×10^{-4}	0.065	19.2	9.88	7.13×10^{-3}
	E	0.925	0.962	1.05×10^{-4}	0.076	20.2	1.24×10^{-2}	0.080
1.6-2.5	PFO	0.734	-0.874	7.52×10^{-3}	1.80	14.8	0.379	5.74
	PSO	0.998	0.999	2.03×10^{-4}	0.130	83.0	12.4	0.087
	W - M	0.783	0.885	5.88×10^{-4}	0.243	32.0	4.29	0.026
	E	0.960	0.980	1.09×10^{-4}	0.060	14.4	1.38×10^{-3}	0.021
2.0-5.0	PFO	0.896	0.901	2.60×10^{-3}	0.761	30.4	1.53	0.827
	PSO	0.990	0.995	1.79×10^{-4}	0.105	89.0	20.4	0.063
	W - M	0.901	0.949	3.91×10^{-4}	0.220	43.3	9.32	0.021
	E	0.887	0.942	3.04×10^{-3}	2.59	145.0	2.04×10^{-4}	0.104

Effect of pH on phosphorus reduction rate

In addition to the aforementioned study of phosphorus sorption kinetics on the Rockfos® material, the effects of pH changes were also analyzed. The initial pH value of the standard solution was 6.28. An increase in pH values was observed for all analyzed fractions during the initial phase of the study, which may present a challenge in terms of the material's suitability for wastewater treatment. In all cases, the maximum values were reached at the same contact time (180 minutes), with the exception of a discrepancy in the values obtained. The maximum pH value for the 1.0–1.6 mm fraction was 9.23, 9.85 for the 1.6–2.5 mm fraction, and 9.76 for the 2.0–5.0 mm fraction (Fig. 4). The pH values were maintained at 8.28–8.42 for contact times of 720 minutes or longer.

During the phase of increasing pH to the maximum level (1–180 minutes), there was a simultaneous increase in the rate of phosphorus sorption, resulting in a reduction in the concentration of this component in solution (Fig. 1, Fig. 4). A review of the data presented in Figures 1 and 4 may indicate a correlation between the rate of phosphorus sorption and the pH value of the solution. The alkalization of the solution during the initial phase of contact with the Rockfos® material can be attributed to the calcination process, which

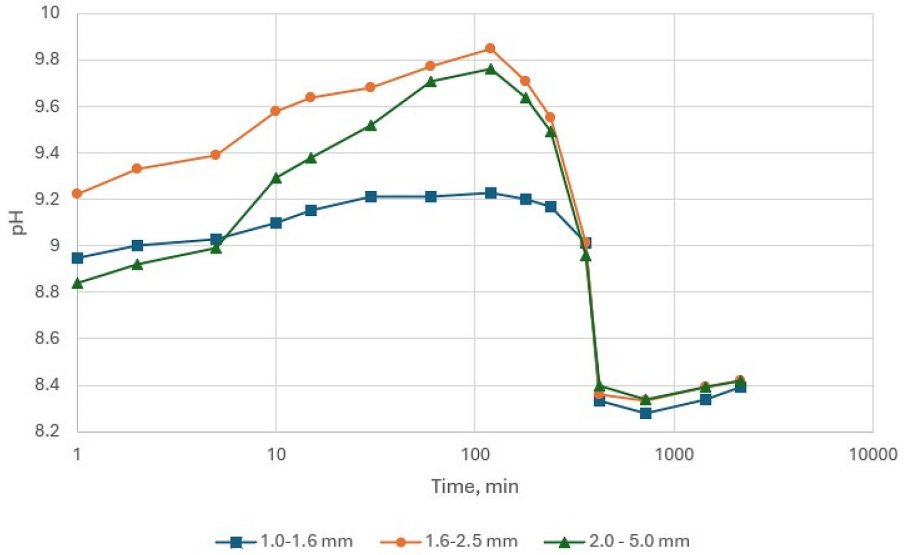

Figure 4. Change of pH value during the study of PO_4^{3-} sorption kinetics on Rockfos® (horizontal axis - logarithmic scale)

results in an increase in the calcium oxide (CaO) content of the material [1, 20, 23]. It is widely held among the scientific community that CaO is the compound most responsible for phosphorus binding [1, 13, 14, 20, 21, 62, 63].

The lowest pH level was achieved at a contact time of 720 minutes, which also coincided with an inhibition of the increase in phosphorus reduction (Fig. 1, Fig. 4). This could indicate a reduction in sorption. Cucarella and Renman also observed comparable outcomes [64].

CONCLUSIONS

Based on the results, the following conclusions can be drawn:

1. The highest phosphorus removal effects were observed for granulations of 2.0–5.0 mm and 1.6–2.5 mm, while the lowest effects were observed for granulations 1.0-1.6 mm. The equilibrium phosphorus removal was observed for all three granulations after 1,440 minutes.
2. The pseudo-second-order kinetic model is a superior fit to the sorption process in the Rockfos® material than the pseudo-first-order model, as evidenced by higher values of the coefficient of determination (R^2) and superior correlation coefficients (r).
3. The kinetics of phosphorus sorption ma Rockfos® material for all analyzed granulations follows the assumptions of pseudo-second-order kinetics, suggesting a chemical nature of sorption, probably involving surface reactions.
4. The equilibrium adsorption capacity obtained from the pseudo-second-order model exhibited the highest values for granulations of 2.0–5.0 mm, while the lowest values were observed for granulations of 1.0-1.6 mm.
5. The values of the rate constant k_2 varied depending on the granulation of the Rockfos® material. The highest value for the pseudo-second-order rate constant was observed for granulations of 1.6–2.5 mm, while the lowest value was observed for granulations of 2.0–5.0 mm.
6. The Weber-Morris and Elovich models are inadequate for providing a definitive account of the impact of Rockfos® material granulation on the phosphorus sorption process.
7. The results of the error analysis demonstrated that the PSO model exhibited the most precise correlation with the measurement outcomes, followed by the Weber-Morris and Elovich models. In this regard, the PFO model is the least effective.
8. The relationship between the pH value and the efficiency of phosphorus sorption on Rockfos® material was demonstrated through a series of controlled experiments. As the degree of reduction in the pH value of the phosphorus solution increased, the solution became more alkaline.
9. The material, with a granulation of 2.0–5.0 mm, has been demonstrated to be effective in wastewater treatment due to its optimal phosphorus removal efficiency and its capacity for equilibrium adsorption.

Acknowledgement

The paper was written within the framework of a Ph.D. thesis prepared by Beata Zawadzka, from the project no DWD/5/0332/2021 financed by the Ministry of Education and Science (Poland) entitled “Development of guidelines for design and operation and implementation of a chemisorption modular phosphorus removal system in a selected wastewater treatment plant”.

REFERENCES

1. Gubernat S, Masłoń A, Czarnota J, Koszelnik P. Reactive materials in the removal of phosphorus compounds from wastewater—A review. Materials. 2020;13(15): 3377.
2. Siwek H, Bartkowiak A, Włodarczyk M. Adsorption of Phosphates from Aqueous Solutions on Alginate/Goethite Hydrogel Composite. Water. 2019; 11(4): 633.
3. Hernández-Navarro C, Pérez S, Flórez E, Acelas N, Muñoz-Saldaña J. Sargassum macroalgae from Quintana Roo as raw material for the preparation of high-performance phosphate adsorbent from aqueous solutions. J Environ Manage. 2023; 342: 118312.
4. Arenas-Montaño V, Fenton O, Moore B, Healy MG. Evaluation of the fertiliser replacement value of phosphorus-saturated filter media. Journal of Cleaner Production. 2021; 291: 125943.
5. Almanassra IW, Kochkodan V, McKay G, Atieh MA, Al-Ansari T. Review of phosphate removal from water by carbonaceous sorbents. J Environ Manage. 2021; 287: 112245.
6. Usman MO, Aturagaba G, Ntale M, Nyakairu GW. A review of adsorption techniques for removal of phosphates from wastewater. Water Science and Technology. 2022; 86(12): 3113–3132.
7. Al-Ghouti MA, Da’ana DA. Guidelines for the use and interpretation of adsorption isotherm models: A review.

Journal of hazardous materials. 2020; 393: 122383.

8. Kong L, Adidharma H. A New Adsorption Model Based on Generalized van der Waals Partition Function for the Description of All Types of Adsorption Isotherms. Chemical Engineering Journal. 2019; 375: 122112.
9. Ayawei N, Ebelegi A, Donbebe W. Modelling and Interpretation of Adsorption Isotherms. Hindawi Journal of Chemistry. 2017; 11.
10. Ramirez-Muñoz A, Pérez S, Flórez E, Acelas N. Recovering phosphorus from aqueous solutions using water hyacinth (Eichhornia crassipes) toward sustainability through its transformation to apatite. Journal of Environmental Chemical Engineering. 2021; 9(5): 106225.
11. Cieślik B, Konieczka P.A review of phosphorus recovery methods at various steps of wastewater treatment and sewage sludge management. The concept of "no solid waste generation" and analytical methods. Journal of Cleaner Production. 2017; 142: 1728–1740.
12. Sørensen BL, Dall OL, Habib K. Environmental and resource implications of phosphorus recovery from waste activated sludge. Waste Manag. 2015; 45: 391–399.
13. Bus A, Karczmarczyk A. Properties of lime-siliceous rock opoka as reactive material to remove phosphorous from water and wastewater. Infrastructure and Ecology of Rural Areas.. 2014(II/1). (in Polish)
14. Jóźwiakowski K, Gajewska M, Pytka A, Marzec M, Gizińska-Górna M, Jucherski A, et al. Influence of the particle size of carbonate-siliceous rock on the efficiency of phosphorous removal from domestic wastewater. Ecological Engineering. 2017; 98: 290–296.
15. Kasprzyk M, Gajewska M. Phosphorus removal by application of natural and semi-natural materials for possible recovery according to assumptions of circular economy and closed circuit of P. Science of the Total Environment. 2019;650:249-56.
16. Kacprzak MJ, Sobik-Szołtysek J. The opoka-rock in N and P of poultry manure management according to circular economy. Journal of Environmental Management. 2022; 316: 115262.
17. Kasprzyk M, editor Treatment Wetland effluent quality improvement by usage sorbents of various origin. E3S Web of Conferences; 2019: EDP Sciences.
18. http://www.ceramika-kufel.pl/rockfos/ (Accessed: 10.05.2024).
19. Renman A, Renman G. Long-term phosphate removal by the calcium-silicate material Polonite in wastewater filtration systems. Chemosphere. 2010; 79(6): 659–664.
20. Jucherski A, Walczowski A, Bugajski P, Jóźwiakowski K, Rodziewicz J, Janczukowicz W, et al. Long-term operating conditions for different sorption materials to capture phosphate from domestic wastewater. Sustainable Materials and Technologies. 2022; 31: e00385.
21. Kasprzyk M, Węgler J, Gajewska M, editors. Analysis of efficiency of phosphates sorption by different granulation of selected reactive material. E3S Web of Conferences; 2018: EDP Sciences.
22. Kasprzyk M, Czerwionka K, Gajewska M. Waste materials assessment for phosphorus adsorption toward sustainable application in circular economy. Resources, Conservation and Recycling. 2021; 168: 105335.
23. Pytka-Woszczyło A, Różańska-Boczula M, Gizińska-Górna M, Marzec M, Listosz A, Jóźwiakowski K. Efficiency of filters filled with rockfos for phosphorus removal from domestic sewage. Advances in Science and Technology Research Journal. 2022; 16(4): 176–188.
24. Zawadzka B, Siwiec T, Marzec M, Jóźwiakowski K, Listosz A. Meandering Flow Filter for Phosphorus Removal as a Component of Small Wastewater Treatment Plants—A Case Study. Water. 2023; 15(15): 2703.
25. ISO P. 6878 Water Quality—Determination of Phosphorus—Spectrometric Method with Ammonium Molybdate. Polish Committee for Standardization: Warszawa, Poland. 2006.
26. ISO P. 10523 Water quality - Determination of pH. Polish Committee for Standardization: Warszawa, Poland. 2012.
27. Wawrzkiewicz M. Removal of C.I. Basic Blue 3 dye by sorption onto cation exchange resin, functionalized and non-functionalized polymeric sorbents from aqueous solutions and wastewaters. Chemical Engineering Journal. 2013; 217: 414–425.
28. Nastawny M, Jucherski A, Walczowski A, Jóźwiakowski K, Pytka A, Gizińska-Górna M, et al. Preliminary evaluation of selected mineral adsorbents used to remove phosphorus from domestic wastewater. Chemical Industry. 2015;94(10): 1762–1766. (in Polish)
29. Zamparas M, Gianni A, Stathi P, Deligiannakis Y, Zacharias I. Removal of phosphate from natural waters using innovative modified bentonites. Applied Clay Science. 2012; 62: 101–106.
30. Huang W, Yu X, Tang J, Zhu Y, Zhang Y, Li D. Enhanced adsorption of phosphate by flower-like mesoporous silica spheres loaded with lanthanum. Microporous and Mesoporous Materials. 2015; 217: 225–232.
31. Liu X, Zhang L. Removal of phosphate anions using the modified chitosan beads: Adsorption kinetic, isotherm and mechanism studies. Powder Technology. 2015;2 77: 112–119.
32. Campos NF, Barbosa CM, Rodríguez-Díaz JM, Duarte MM. Removal of naphthenic acids using activated charcoal: Kinetic and equilibrium studies. Adsorption Science & Technology. 2018: 36(7–8): 1405–1421.
33. Saoudi Hassani EM, Azzouni D, Alanazi MM,

Mehdaoui I, Mahmoud R, Kabra A, et al. Innovative plant-derived biomaterials for sustainable and effective removal of Cationic and Anionic dyes: kinetic and thermodynamic study. Processes. 2024; 12(5): 922.

34. Tsibranska I, Hristova E. Comparison of different kinetic models for adsorption of heavy metals onto activated carbon from apricot stones. Bulgarian Chemical Communications. 2011;43(3): 370-7.
35. Zamri NII, Zulmajdi SLN, Daud NZA, Mahadi AH, Kusrini E, Usman A. Insight into the adsorption kinetics, mechanism, and thermodynamics of methylene blue from aqueous solution onto pectin-alginate-titania composite microparticles. SN Applied Sciences. 2021; 3: 1–16.
36. Gupta SS, Bhattacharyya KG. Adsorption of Ni (II) on clays. Journal of colloid and interface science. 2006; 295(1): 21–32.
37. Wu F-C, Tseng R-L, Juang R-S. Characteristics of Elovich equation used for the analysis of adsorption kinetics in dye-chitosan systems. Chemical Engineering Journal. 2009; 150(2–3): 366–373.
38. Wang L, Zhang J, Zhao R, Li Y, Li C, Zhang C. Adsorption of Pb (II) on activated carbon prepared from Polygonum orientale Linn.: kinetics, isotherms, pH, and ionic strength studies. Bioresource technology. 2010; 101(15): 5808–5814.
39. Hamdaoui O, Saoudi F, Chiha M, Naffrechoux E. Sorption of malachite green by a novel sorbent, dead leaves of plane tree: Equilibrium and kinetic modeling. Chemical engineering journal. 2008; 143(1–3): 73–84.
40. Largitte L, Pasquier R. A review of the kinetics adsorption models and their application to the adsorption of lead by an activated carbon. Chemical engineering research and design. 2016;109:495-504.
41. Chutkowski M, Petrus R, Warchol J, Koszelnik P. Sorption equilibrium in processes of metal ion removal from environment. Statistical verification of mathematical models. Przemysl Chemiczny. 2008; 87(5): 436–438.
42. Ho Y-S, Chiu W-T, Hsu C-S, Huang C-T. Sorption of lead ions from aqueous solution using tree fern as a sorbent. Hydrometallurgy. 2004;73(1-2):55-61.
43. Ho Y-S, McKay G. Pseudo-second order model for sorption processes. Process biochemistry. 1999; 34(5): 451–65.
44. Bus A. Assessment of sorption properties and kinetic reaction of phosphorus reactive material to limit diffuse pollution. Annals of Warsaw University of Life Sciences-SGGW Land Reclamation. 2017; 49(3).
45. Eljamal O, Okawauchi J, Hiramatsu K, Harada M. Phosphorus sorption from aqueous solution using natural materials. Environmental earth sciences. 2013; 68: 859–863.
46. Osama E, Junya O, Kazuaki H. Removal of phosphorus from water using marble dust as sorbent material. Journal of Environmental Protection. 2012; 2012.
47. Riahi K, Chaabane S, Thayer BB. A kinetic modeling study of phosphate adsorption onto Phoenix dactylifera L. date palm fibers in batch mode. Journal of Saudi Chemical Society. 2017;21:S143-S52.
48. Özacar M. Equilibrium and kinetic modelling of adsorption of phosphorus on calcined alunite. Adsorption. 2003; 9: 125–132.
49. Letshwenyo MW, Mokokwe G. Phosphorus and sulphates removal from wastewater using copper smelter slag washed with acid. SN Applied Sciences. 2021; 3: 1–18.
50. Guo H, Qin Q, Chang J-S, Lee D-J. Modified alginate materials for wastewater treatment: Application prospects. Bioresource Technology. 2023;387:129639.
51. Gao X, Guo C, Hao J, Zhao Z, Long H, Li M. Adsorption of heavy metal ions by sodium alginate based adsorbent-a review and new perspectives. Int J Biol Macromol. 2020; 164: 4423–4434.
52. Fu L, Li J, Wang G, Luan Y, Dai W. Adsorption behavior of organic pollutants on microplastics. Ecotoxicol Environ Saf. 2021; 217: 112207.
53. Brogowski Z, Renman G. Characterization of opoka as a basis for its use in wastewater treatment. Polish Journal of Environmental Studies. 2004; 13(1): 15–20.
54. Cucarella V, Zaleski T, Mazurek R. Phosphorus sorption capacity of different types of opoka. Annals of Warsaw University of Life Sciences-SGGW Land Reclamation. 2007(38): 11–18.
55. Johansson L. Industrial by-products and natural substrata as phosphorus sorbents. Environmental technology. 1999; 20(3): 309–316.
56. Nilsson C. Phosphorus removal in reactive filter materials: factors affecting the sorption capacity: KTH Royal Institute of Technology; 2012.
57. Jóźwiakowski K. Experiment of increasing effectiveness of phosphorus removal in a model of wastewater treatment plant. Agricultural Engineering. 2006; 10(5)(80): 249–56. (in Polish)
58. Johansson L, Hylander L. Phosphorus removal from waste water by filter media: Retention and estimated plant availability of sorbed phosphorus. Problematic Notebooks of the Progress of Agricultural Sciences. 1998;458.
59. López-Luna J, Ramírez-Montes LE, Martinez-Vargas S, Martínez AI, Mijangos-Ricardez OF, González-Chávez MdCA, et al. Linear and nonlinear kinetic and isotherm adsorption models for arsenic removal by manganese ferrite nanoparticles. SN Applied Sciences. 2019; 1: 1–19.
60. Ho Y-S. Review of second-order models for adsorption systems. Journal of hazardous materials.

2006;136(3): 681–689.

61. Dada A.O, Adekola F.A, Odebunmi E.O, Ogunlaja AS, Bello OS. Two–three parameters isotherm modeling, kinetics with statistical validity, desorption and thermodynamic studies of adsorption of Cu (II) ions onto zerovalent iron nanoparticles. Scientific reports. 2021; 11(1): 16454.
62. Jucherski A, Nastawny M, Walczowski A, Jóźwiakowski K, Gajewska M. Testing the suitability of alkaline filter materials for phosphate removal from biologically treated domestic wastewater. Environmental Protection. 2017; 39(1). (in Polish)
63. Westholm LJ. Substrates for phosphorus removal—Potential benefits for on-site wastewater treatment? Water research. 2006; 40(1): 23–36.
64. Cucarella V, Renman G. Phosphorus sorption capacity of filter materials used for on-site wastewater treatment determined in batch experiments–a comparative study. Journal of environmental quality. 2009; 38(2): 381–392.